LWT - Food Science and Technology 44 (2011) 1291–1302

Contents lists available at ScienceDirect

LWT - Food Science and Technology

journal homepage: www.elsevier.com/locate/lwt

Microstructure of milk gel and cheese curd observed using cryo scanning electron microscopy and confocal microscopy

Lydia Ong [a,b], Raymond R. Dagastine [a], Sandra E. Kentish [a], Sally L. Gras [a,b,*]

[a] Particulate Fluids Processing Centre, Department of Chemical and Biomolecular Engineering, The University of Melbourne, Parkville, Victoria 3010, Australia
[b] The Bio21 Molecular Science and Biotechnology Institute, The University of Melbourne, Parkville, Victoria 3010, Australia

ARTICLE INFO

Article history:
Received 23 June 2010
Received in revised form
20 December 2010
Accepted 24 December 2010

Keywords:
Cheddar
Processing
Homogenised
Optimisation

ABSTRACT

Cryo scanning electron microscopy (cryo SEM) and confocal laser scanning microscopy (CLSM) were used to visualise changes in the microstructure of milk, rennet-induced gel and curd during the manufacture of Cheddar cheese. Our results show that cryo preservation did not alter the microstructure of the sample when it was fixed by rapid freezing in slush liquid nitrogen due to the formation of amorphous ice. Artefacts such as the formation of ice crystals could be observed in samples when immersed directly into liquid nitrogen (−196 °C) at atmospheric pressure. These ice crystals changed the shape of sample pores increasing their size to >20 μm. The etching time, thickness of gold coating, accelerating voltage and type of detector used for cryo SEM observation were varied in order to minimise the formation of such artefacts and optimise conditions for imaging. Chains and clusters of casein micelles and fat globules were best observed in the gel and the cooked curd when the samples were freeze fractured and etched for 30 min, coated with a mixture of gold and palladium alloy approximately 6 nm thick at −140 °C and observed using a backscattered electron detector at 15 kV. The structure of the gel, curd and cheese was also observed using CLSM. Spherical fat globules were mostly present in the serum pores of the gel prepared from unhomogenised milk but were found embedded in the aggregated chains of the casein network within the gel prepared from homogenised milk when observed using CLSM. The porosity measurements obtained using cryo SEM were similar to those obtained using CLSM. These two complementary techniques can potentially be used to assist studies for the control of cheese texture and functionality.

© 2011 Elsevier Ltd. All rights reserved.

1. Introduction

Many of the properties of cheese such as cheese texture and flavour are determined by the spatial arrangement of components including: the casein particles that form a protein matrix, the fat globules, dispersed water and minerals (Everett, 2007). The arrangement of these components on the micron scale is known as the microstructure of cheese. In Cheddar cheese, this microstructure develops when milk coagulates to form a gel, usually through the enzymatic action of chymosin. Changes in process conditions or the choice of ingredients can alter the microstructure of the gel, curd and cheese considerably and thus the functional properties of the final cheese product. The ability to image and characterise these changes will provide an important tool for the quality control of cheese and other dairy products.

A number of studies describe the use of transmission electron microscopy (TEM) (Kheadr, Vachon, Paquin, & Fliss, 2002), scanning electron microscopy (SEM) (Fallico et al., 2006; Kimber, Brooker, Hobbs, & Prentice, 1974; McMahon, Fife, & Oberg, 1999) and cryo scanning electron microscopy (cryo SEM) (Hassan, Frank, & Elsoda, 2003; Mistry, Hassan, & Acharya, 2006) to examine the microstructure of the final cheese product. A limited number of studies have also looked at the microstructure of intermediate samples collected during cheese manufacture such as the gel and/or cooked curd using light microscopy (Bowland & Foegeding, 2001; Lagaude, Fernandez, Cuq, & Marchesseau, 2004), fluorescence microscopy (Yiu, 1985), confocal laser scanning microscopy (CLSM) (Auty, Twomey, Guinee, & Mulvihill, 2001; Heilig, Göggerle, & Hinrichs, 2009; Oiseth & McKinnon, 2006), SEM (Kalab & Harwalkar, 1973; Merrill, Oberg, McManus, Kalab, & McMahon, 1996) and cryo SEM (Mellema, Walstra, can Opheusden, & van Vliet, 2002). Reviews of these techniques have highlighted the potential use of cryo SEM for

Abbreviations: CLSM, confocal laser scanning microscopy; SEM, scanning electron microscopy; TEM, transmission electron microscopy; ETD, Everhart Thornley detector; SSD, solid state detector.

* Corresponding author. The Bio21 Molecular Science and Biotechnology Institute, The University of Melbourne, Parkville, Victoria 3010, Australia. Tel.: +61 3 8344 6281; fax: +61 3 8344 4153.
E-mail address: sgras@unimelb.edu.au (S.L. Gras).

0023-6438/$ – see front matter © 2011 Elsevier Ltd. All rights reserved.
doi:10.1016/j.lwt.2010.12.026

the observation of highly hydrated food samples (Everett & Auty, 2008; James, 2009; Kalab, Allan-Wojtas, & Miller, 1995).

SEM has been widely used to study the microstructure of cheese products without cryo preservation but this method has several disadvantages (Fallico et al., 2006; Kimber et al., 1974; McMahon et al., 1999). A scanning electron microscope operates under high vacuum ($\sim 10^{-4}$ Pa) and extensive sample preparation is required prior to analysis due to the high moisture and fat content of cheese. Dehydration is required to prevent water vaporising within the microscope chamber. Fat and other volatiles should also be fixed or extracted to avoid melting when the sample is under the electron beam. These modifications can change the microstructure and increase the possibility of artefacts, making data interpretation difficult (Hassan et al., 2003). Some of these problems can be overcome with Environmental Scanning Electron Microscopy (ESEM). This technique has been used to observe the microstructure of reduced fat imitation cheese without significant preparation or a metallic coating (Noronha et al., 2008). ESEM differs from conventional SEM in that samples can be imaged in their hydrated state in the presence of water vapour. However, there are limitations with this technique including a slight degradation of image quality (Donald, 2003) and obstructions caused by the presence of water preventing the effective observation of the protein matrix and pores (Noronha et al., 2008).

The cryogenic preservation and imaging of samples are growing in popularity as an alternative to traditional SEM. However, studies investigating the microstructure of rennet gels using cryo SEM have been mainly limited to skim milk models. Cryo SEM relies on the formation of a non-crystalline form of ice. When water is cooled slowly at temperatures above −70 °C and at atmospheric pressure, the basic tetrahedron structure of water is maintained and it becomes extensively linked into hexagonal crystals that distort the sample, displacing casein micelles and altering the sample microstructure (Kuoa & Gunasekaran, 2009; Riberoa, Rubioloa, & Zorrilla, 2009). Two additional types of ice may form at atmospheric pressure including amorphous ice, also known as vitreous ice, and cubic ice. Amorphous ice is a glass-like solid that is non-crystalline and cubical ice forms when this amorphous ice is warmed.

During cryo preservation, hydrated samples are stabilised by rapid freezing in a nitrogen slush at −210 °C, producing amorphous ice (Kasas, Dumas, Dietler, S. & Adrian, 2003). This technique has been shown to preserve the fine microstructure of hydrated samples such as yoghurt (Amatayakul, Sherkat, & Shah, 2006), rennet-induced gels (Mellema et al., 2002), Cheddar cheese (Mistry et al., 2006) or Karish and Feta cheeses (Hassan et al., 2003). In addition, the sample can be freeze fractured under cryogenic conditions exposing the internal microstructure. Etching can then be used to remove water from the sample in a controlled manner revealing further internal structural detail. Consequently cryogenic preparation is expected to give the best possible chance of viewing the microstructure of highly hydrated sample components in their natural state compared to other dehydrating techniques, though sample preparation is critical to minimise the formation of artefacts.

CLSM has also been used to examine cheese microstructure, one of the advantages of this technique is that it can both visualise and chemically differentiate cheese components through the use of protein and lipid specific stains. The tryptophan residues and vitamin A in milk may be considered intrinsic fluorescent probes for proteins and lipids respectively (Herbert, Bouchet, Riaublanc, Dufour, & Gallant, 1999), however, these probes cannot be excited using the lasers typically installed on commercial confocal microscopes. Consequently extrinsic fluorechromes must be used such as acridine orange, Nile blue, fluorescein isothiocyanate (FITC), rhodamine B and fast green FCF to stain protein and BODIPY® Nile red to stain fat (Auty et al., 2001; Heilig et al., 2009; Lopez, Camier, & Gassi, 2007; Lorén, Langton, & Hermansson, 2007; Mounsey & O'Riordan, 2008; Oiseth & McKinnon, 2006; Zisu & Shah, 2005). The optical sectioning capability of CLSM has proved very useful in the examination of high-fat foods, which are difficult to prepare using the conventional microscopy without the loss or migration of fat globules.

The first aim of this study was to investigate several sample preparation parameters including the freezing method, the etching time, thickness of metal coating, acceleration voltage and type of detector used for SEM observation with an aim to minimise the formation of artefacts. The potential of cryo SEM was also assessed as a technique to visualise the microstructure of the highly hydrated gel, curd and cheese samples collected during Cheddar cheese manufacture using homogenised or unhomogenised milk. A further aim was to follow the development of microstructure during the manufacture of Cheddar cheese using CLSM and to compare qualitative and quantitative data obtained by cryo SEM and CLSM.

2. Material and methods

2.1. Manufacture of Cheddar cheese

A total of six batches of Cheddar cheese were made in three independent trials. In each trial, two batches of cheese were prepared with 4 L of unhomogenised or homogenised milk and 0.05 g/L of freeze dried mixed strain direct vat set (DVS) starter culture, *Lactococcus lactis* subsp. *lactis* and *L. lactis* subsp. *cremoris* (Chr. Hansen, Bayswater, Vic, Australia). The unhomogenised milk was prepared for cheese manufacture by Murray Goulburn (Cobram, Vic, Australia), defined here as cheese-milk. This milk had been pasteurised (72 °C for 15 s) and standardised to a fat composition of 45 ± 0.7 g/L and protein composition of 38 ± 0.8 g/L. The homogenised milk was from a commercial source, which had been pasteurised and contained 34 ± 1 g/L fat and 32 ± 0.8 g/L protein (Devondale; Murray Goulburn, Brunswick, Vic, Australia). The milk was tempered to 33 °C before inoculation with the starter culture. A stock of starter culture was prepared from the freeze-dried starter (1 g) and diluted into a milk sample (10 mL) at 40 °C for 15 min before addition to the tempered milk at a concentration of 0.5 mL/L milk. When the pH of the milk reached 6.60, rennet (Hannilase, 690 IMCU/mL; Chr. Hansen) was added (0.1 mL/L of milk). The milk was allowed to coagulate for a period of 45 min at 33 °C. The resultant gel was then cut with a cheese wire knife into 1 cm cubes. The gel was cooked by heating the curd slowly from to 33 °C to 38 °C at a rate of 1 °C rise per 12 min with gentle stirring at 5 revolutions per minute for 60 min. The temperature was then kept constant at 38 °C for a further 30 min or until the pH dropped to 6.1. The whey was drained and the cooked curd was cheddared at 38 °C and turned every 15 min until the pH dropped to 5.4. The cheddared curd was milled (generating pieces of 1–2 cm^3) and dry salted 30 g/L before the curds were placed manually into a cheese mould and pressed for 16 h. A pressure equivalent to 25 g/cm^2 was used to press the curd. The weight applied was calculated by clamping the cheese press over a weight balance (Soehnle; Leifheit AG, Nassau, Germany). The pressed curd or the cheese (477 ± 6 g) was removed from the mould and stored at 4 °C in a zip lock plastic bag from which the air had been removed. The gel and curd samples were analysed immediately after sampling, while the cheese samples were analysed within one week of pressing.

2.2. Cryo scanning electron microscopy

The cryo sample preparation system (Alto 2500; Gatan, Abingdon, Oxon, U.K.) has three main components: a slushing station, a vacuum transfer device (VTD) and a sample preparation chamber

(Fig. 1). The gel, cooked curd and cheese samples were prepared for cryo SEM by mounting on a copper holder with Tissue-Tek (OCT Compound; ProSciTech). The copper holder was attached to the VTD that fits directly onto the slushing chamber.

Fresh samples were rapidly immersed into liquid nitrogen slush (a mixture of solid and liquid nitrogen at its freezing point (−210 °C)). The liquid nitrogen used was freshly filled to prevent the presence of particulates that may provide nucleation for the growth of ice crystals. To make the nitrogen slush, the liquid nitrogen was filled into a polystyrene cup that was then placed in the slushing chamber. The chamber was then evacuated using a rotary pump until, through a loss of latent heat of evaporation, the nitrogen ceased to bubble and solidified. After 30 s, the vacuum was released to allow for the solidified nitrogen to melt. The process was repeated twice to ensure that the entire volume of the nitrogen was brought to its freezing temperature (−210 °C) ready for use. The samples were rapidly immersed into the freshly prepared slush for 15 s. For comparative purposes, a rennet-induced gel made from unhomogenised milk was also immersed directly into liquid nitrogen (b.p. −196 °C).

Following freezing the frozen specimens were immediately transferred using the VTD into an attached cryo preparation chamber. The VTD allows for sample to be transferred under vacuum ($>10^{-4}$ Pa) to the sample preparation chamber to prevent ice recrystallisation (the growth of smaller ice crystals to a larger size) and thus minimise any changes in microstructure. With the aid of an externally fitted binocular microscope, the sample was fractured using a chilled scalpel blade in the chamber which was maintained at −140 °C under a high vacuum condition ($>10^{-4}$ Pa). The specimen was then etched (facilitating the removal of ice from the surface of the fractured sample by vacuum sublimation) at −95 °C for 5 min, 15 min, 30 min, 45 min or 60 min and coated using a cold magnetron sputter coater with 300 V, 10 mA of sputtered gold/palladium alloy (60/40) for 60 s (~3 nm) or 120 s (~6 nm). It was then transferred under vacuum onto a nitrogen gas cooled module, maintained at −140 °C and observed using a field emission gun SEM (Quanta; Fei Company, Hillsboro, Oregon, U.S.A.) at 5.0 kV, 7.5 kV, 10 kV or 15 kV. The detectors used for the SEM observation were an Everhart Thornley detector (ETD) and a solid state detector (SSD).

2.3. Confocal laser scanning microscopy

The gel sample for CLSM observation was prepared during the cheese making process as previously reported in Ong, Dagastine, Kentish, and Gras (2010). The cooked and cheddared curd samples were collected from the cheese vat during the cheese making process. The cheese sample was collected after 16 h of pressing. The samples were cut into thin strips approximately 10 mm × 10 mm × 2 mm in size. A surgical blade was used to minimise distortion of the surface. Staining was performed at 4 °C

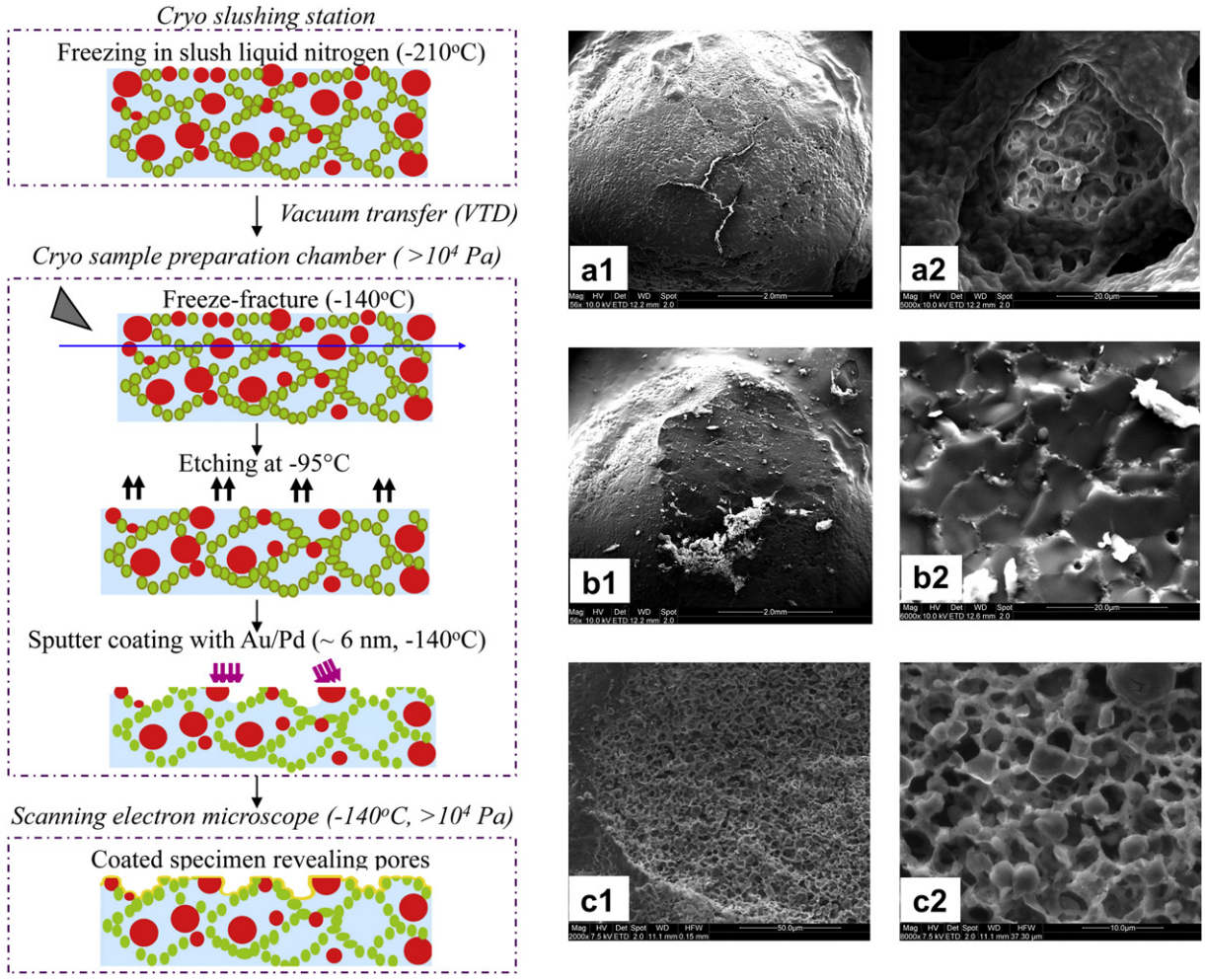


Fig. 1. Sample preparation methods for cryo scanning electron microscopy are shown on the left (● = fat globule; ● = protein and □ = pore). The cryo SEM micrographs of gel after slush freezing (a1–a2), freeze fracturing (b1–b2) and etching (c1–c2) are shown on the right. Images were captured using a Everhart Thornley detector. The scale bars are 2 mm (a1, b1), 20 μm (a2, b2), 50 μm (c1) or 10 μm (c2) in length.

to prevent the mobility of liquid fat, which could result in fat coalescence and large fat globules rising to the coverslip surface. The lipid specific stain Nile red was prepared from a stock solution of Nile red (1 mg/mL, containing 0.5 mL/L dimethylsulfoxide (DMSO, Sigma–Aldrich)) and dissolved in simulated milk ultrafiltrate solution (SMUF) just prior to staining to a final concentration of 0.02 mg/mL. The protein-specific stain fast green FCF (Sigma–Aldrich) was dissolved in SMUF solution to a final concentration of 0.1 mg/mL. The curd and cheese samples were soaked in the mixed protein and lipid stains for 10 min before washing with purified water (Millipore, Billerica, MA, US; purified to a resistivity of 18.2 mΩ). The fluorescently labelled curd and cheese slices were placed on a microscope slide (ProSciTech, Thuringowa, Queensland, Australia), mounted with glycerol based anti-fading agent (~15 μL) (AF2; Citifluor Ltd., Leicester, London, U.K.) and secured with a glass coverslip (0.17 mm thick) (ProSciTech).

The sample was then inverted for observation using an inverted confocal laser scanning microscope (Leica TCS SP2; Leica Microsystems, Heidelberg, Baden-Württemberg, Germany) powered by Ar/Kr and He/Ne lasers. The sample was viewed using an oil immersion 63 × lens (1.32 Numerical Aperture) and the pinhole diameter was maintained at 1 Airy unit. Nile red was excited at a wavelength of 488 nm and fast green FCF at 633 nm. The emission filters were set at 555–620 nm for Nile red and 660–710 nm for fast green FCF. Images were recorded at a depth of 10–20 μm from the surface of the glass coverslip. Leica confocal software was used to acquire digital images 464 pixels × 460 pixels in size that were the average of 8 frames.

2.4. Image analysis

Image analysis of cryo SEM and CLSM micrographs was performed using ImageJ software (Research Services Branch, National Institute of Health, Maryland, U.S.A.) equipped with a 'Pore Analysis' and 'ComputeStat' plug-ins as previously reported in Ong et al. (2010). The images were enhanced and flattened using a bandpass filter. The enhanced image was then transformed to a binary imaged using an Otsu thresholding algorithm automatic binarisation with all structural features contributing black pixels and all background features contributing white pixels (Impoco, Carrato, Caccamo, Tuminello & Licitra, 2006).

The porosity was calculated as the fraction of pore area with respect to the total sample area (0.002 mm^2). The porosity calculated here is only equal to a two-dimensional pore fraction and not the absolute porosity of the sample. However it provides a quantitative comparison of micrographs obtained from different samples. The ImageJ program 'Analyze Particle' was used to measure the mean area of the milk fat globules (the mean area per fat globule measured across all fat globules within the total sample area) observed using CLSM. The fat globule diameter was then calculated from the mean area of the milk fat globule and expressed as the number-area mean $D_{FG}[2,0]$ where the mean diameter $= (\Sigma d^2)/n$ (Rawle, 2002).

2.5. Data analysis

Quantitative results are expressed throughout this report as the mean ± the standard deviation of data obtained from three gel, curd or cheese samples. A large number of globules were analysed for each curd and cheese sample using ImageJ (~300–800 fat globules), with the exact number dependant on the number of fat globules present in the sampling area for both CLSM and cryo SEM micrographs. The sampling area for cryo SEM micrographs was normalised to a sample area of 0.002 mm^2, equivalent to the total sample area imaged by CLSM, to enable comparisons between data obtained from the two techniques. Data analysis was carried out using a statistical package from Minitab (Minitab Inc, State College, PA, USA). One way analysis of variance (ANOVA) and Tukey's paired comparison were used to study the difference between means, with a significance level of $\alpha = 0.05$.

3. Results and discussion

3.1. Microstructure observation using cryo scanning electron microscopy

We first set out to assess the feasibility of using cryo SEM to study the microstructure of the gel, curd and cheese for a model Cheddar cheese system and to optimise sample preparation and microscope settings for these samples. Fig. 1 presents the protocol used for the cryo preparation of rennet-induced gel made using unhomogenised milk collected during Cheddar cheese making. The gel sample was fixed by rapid freezing in liquid nitrogen slush (−210 °C). After rapid freezing, the microstructure such as the protein network was only visible through the holes of the frozen gel (Fig. 1a2). The internal microstructure could be revealed after freeze fracturing (Fig. 1b) and etching of the amorphous ice (Fig. 1c). All samples were sputter coated with a mixture of Au/Pd (60/40) before observation using SEM. A fine interconnected protein structure could be observed with fat globules attached to the protein network, indicating that this technique provides useful insight into product structure during the intermediate stages of manufacture.

3.1.1. Freezing and freeze-fracturing condition

The importance of the conditions used for sample freezing was assessed by immersing the rennet-induced gel directly into liquid nitrogen (without slushing). Under these conditions the shape of the pores within the gel sample changed, as shown in Fig. 2. Rectangular pores with a width of approximately 20 μm were observed indicating damage to the gel microstructure due to the formation of ice crystals. The position of fat globules within the network was also altered and most globules appeared attached to the sides of the pores (Fig. 2b, c), possibly due to the growth of large ice crystals. According to Severs, Terence, and Shotton (1995), heat transfer from a warm sample immersed directly into liquid nitrogen at its boiling point (−196 °C) is limited by an insulating layer of evaporated nitrogen gas, commonly known as the Leidenfrost effect. The maximum freezing rate is therefore only $\sim 10^3$ °C/s, which allows the growth of large ice crystals that may damage the gel microstructure. In contrast, rapid freezing results in vitreous or amorphous ice that better preserves sample microstructure.

The formation of amorphous ice can be achieved at atmospheric pressure if the sample is cooled at a rate greater than $\sim 10^5$ °C/s (Severs et al., 1995). This rate of cooling can only be achieved for very thin samples that are rapidly plunged into liquid cryogens. In our experiment, the rapid freezing was performed in a liquid nitrogen slush (−210 °C). The sample was approximately 5 mm in width, 2 mm in depth and 2 mm height, as samples of smaller size may be mechanically disrupted due to the fragile nature of the gel. Vitrification might not be achieved throughout the specimen depth, since the maximal cooling rate is limited by heat transfer within the sample. Consequently observations were performed within 100 μm of the surface at the edge of the fracture (Fig. 1c) where cooling is expected to be rapid. It is interesting to note, however, that no obvious changes in the microstructure of the pores were observed beyond a depth of 100 μm (data not shown). It is possible that crystalline ice did form within the pores at greater depths within the sample but that the size of the ice crystals was smaller than the size of the pores resulting in limited changes to the microstructure.

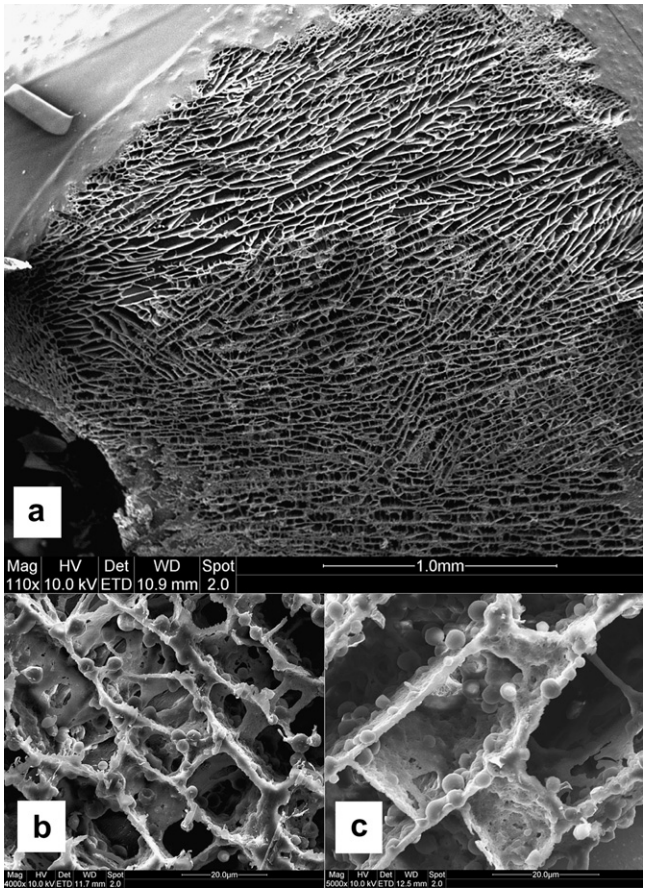


Fig. 2. Cryo scanning electron microscopy images of the gel prepared from unhomogenised milk after direct immersion of the sample in liquid nitrogen at atmospheric pressure. Images were captured using a Everhart Thornley detector. The scale bars are 1 mm (a) or 20 μm (b, c) in length.

Several studies have suggested the use of high pressure freezing to improve the freezing rate of the sample and promote the formation of amorphous ice (Gilkey & Staehelin, 1986; Sartori, Richter, & Dubochet, 1993). No ice crystal damage is apparent to a depth of 600 μm in planar samples and to a depth of 1 mm in spherical samples using this technique (Gilkey & Staehelin, 1986). Sartori et al. (1993) also reported true vitrification to an average depth of 200 μm at high pressure. Disadvantages of this technique include the cost and a lack of mechanism for the direct vacuum transfer of samples to the SEM chamber. Manual transfer will increase the chance of contamination and if the specimen thaws at this stage slow ice recrystallisation can occur which will change the microstructure of the sample.

In our study, the frozen sample was freeze fractured at −140 °C under vacuum ($>10^4$ Pa) using a sharp cold blade to minimise marks on the fracture plane due to friction between the knife and the specimen. Etching was performed following freeze fracture by slightly raising the temperature of the frozen specimen to −95 °C so that water molecules sublime from the surface. It is important to note that ice recrystallisation and the formation of cubic ice may occur during the etching process (Severs et al., 1995). For example, water molecules subliming from the surface of the sample may re-condense onto the sample contaminating the cold fracture surface. This phenomenon was avoided by providing a cold trap around the specimen. The sample preparation chamber is also equipped with an anti-contaminator (liquid nitrogen cooled to <−160 °C). This allows the sublimed water to preferentially condense onto the anti-contaminator preventing condensation on the sample.

3.1.2. Etching condition

The etching temperature (−95 °C) was also carefully selected. Previously, no significant differences in gross topography were observed when the specimen had been fractured at temperatures between −93 °C and −269 °C (Abeysekera & Robards, 1995). When the sample was etched above −90 °C, there were changes on the surface morphology, including the loss of surface details, extreme surface roughening and the appearance of holes in the sample (Davy & Branton, 1970).

The effect of etching duration (5 min, 15 min, 30 min, 45 min and 60 min at −95 °C using a cold trap <−160 °C) on the microstructure within gels prepared using unhomogenised milk was assessed as shown in Fig. 3. The pores and fat globules were partially covered by ice after 5 min (Fig. 3a1–a2), preventing the location of individual pores and fat globules. After etching for 15 min, the porous structure of the gel was revealed with round fat globules present within the pores (Fig. 3b1–b2). Increasing the etching time to 30 min revealed the porous structure of the protein network to a greater sample depth (Fig. 3c1–c2). The colloidal structure of the protein network was also more apparent indicating sufficient ice had been removed.

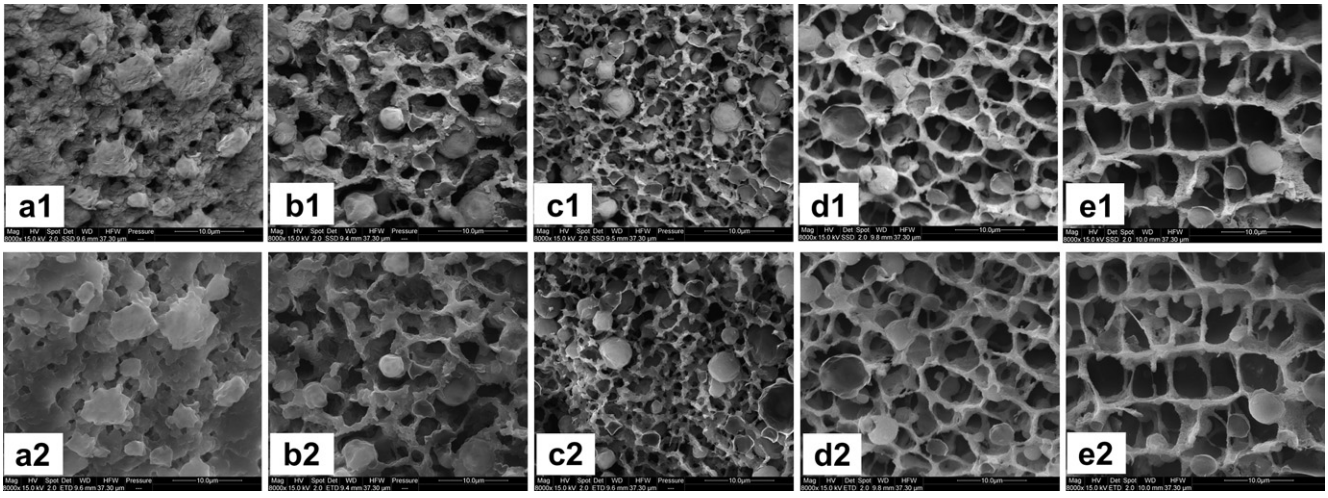


Fig. 3. Cryo scanning electron microscopy images of the gel prepared from unhomogenised milk after etching for 5 min (a1, a2), 15 min (b1, b2), 30 min (c1, c2), 45 min (d1, d2) or 60 min (e1, e2) captured using a solid state backscatter electron detector (a1, b1, c1, d1 and e1) or Everhart Thornley detector (a2, b2, c2, d2 and e2). The scale bars are 10 μm in length.

No evidence of surface roughening, asperities or structure collapse was observed on the etched surface. However, with prolonged sublimation the pore size increased and the protein network was observed to break at 60 min (Fig. 3d and e). An etching time of 30 min was chosen as optimal for the observation of the internal microstructure during Cheddar manufacture. Previously, a shorter etching time of 5–10 min was used for gel, Karish and Feta cheese samples but these samples were made from either skim or low fat milk and the etching temperature was higher (−80 °C). These differences highlight the potential variability of optimum etching conditions with different equipment and different sample type.

3.1.3. Thickness of metal coating, acceleration voltage and type of detector used for SEM

The sample is typically coated with an electrically conductive layer for EM observation. A few factors worth consideration during coating are the sample temperature, coating thickness and size of the coating particles (Yamada et al., 1983). The sample temperature can increase due to radiant heat and electron bombardment resulting in ice recrystallisation. In our experiment, a cold magnetron sputter coater was used to prevent thermal damage. The arrangement of magnets within this coater restricts argon ions to a toroidal ring around the target and deflects high energy electrons generated during glow discharge away from the sample. It also increases ion yield and sputtering efficiency. Coating was performed when the sample preparation chamber equilibrated to −140 °C after completing the etching process.

Materials currently used for coating include gold (Au), gold/palladium alloy (Pd), platinum, osmium, iridium, tungsten, chromium and graphite. Sputter coating with pure gold produces topographic contrast and increases resolution; however, gold produces the largest grain size. This can prevent the observation of colloidal structures such as the protein network in gel and curd samples, making data interpretation difficult. In this study all samples were coated with a ratio of 60:40 Au:Pd. The Pd alloy prevents gold particles from clumping (Yamada et al., 1983) resulting in a fine granularity on cryo SEM images.

The effect of sputter coating duration was assessed on gels prepared using unhomogenised milk (Supplementary material). Sputtering for 60 s and 120 s at a rate of 0.045 nm/s, produced a layer approximately ~3 nm and ~6 nm thick respectively. Artefacts of poor coating such as charging, where static charge accumulates resulting in bright spots on the image, were absent. Both coatings produced images with similar resolution and structural detail with little evidence of over coating which can obscure fine details of the specimen at high magnifications. Our result is similar to a previous study, where sputter coating with 5 nm platinum was found acceptable for cryo SEM observation of a rennet-induced gel (Mellema et al., 2002).

Two types of detectors were used simultaneously for SEM observation (Fig. 3). These were the Everhart Thornley detector (ETD) and solid state detector (SSD). The ETD is sensitive to the secondary electrons (SE) that originate from inelastic collisions between electrons and atoms within the sample. These lower energy electrons are released within a few nanometres from the sample surface and produce a signal rich in topographic information. The SSD is sensitive to backscattered electrons (BSE) reflected from atoms in the specimen by elastic collisions. SSDs are located at a low angle parallel to the sample surface to detect BSE originating from deep within the sample, resulting in a higher contrast image. Heavy elements with a high atomic number backscatter electrons more strongly than light elements, providing contrast between areas of different chemical composition. Images of gels prepared using unhomogenised milk taken with the SSD detector (Fig. 3a1, b1, c1, d1, e1) provide better contrast than those taken with the ETD detector (Fig. 3a2, b2, c2, d2, e2). This enhanced contrast is particularly useful for image analysis and the SSD detector was used for all subsequent image capture.

The influence of microscope acceleration voltage on the clarity of the cryo SEM images was also investigated (Supplementary material). When the sample was observed at lower acceleration voltages, greater structural detail was observed but the image was out of focus. Increasing the acceleration voltage increase the clarity of the image and an acceleration voltage of at least 10 kV was selected to provide a better visualisation of the sample microstructure.

In summary, the optimum conditions for the preparation and observation of gels made from unhomogenised milk during Cheddar manufacture were rapid freezing in a liquid nitrogen slush (−210 °C), etching at −95 °C for 30 min, coating with an Au/Pd alloy to create a surface layer between 3 nm and 6 nm thick, followed by observation within 100 μm of the sample edge with an accelerating voltage of at least 10 kV using a solid state detector.

3.2. Comparison of cryo SEM and confocal images

We next applied the settings for optimised sample preparation and observation by cryo SEM to compare the microstructure of the gel, cooked curd and cheese (Figs. 4 and 5) with the microstructure observed using CLSM (Figs. 6 and 7).

The gel is the product obtained during the initial coagulation of milk. A number of factors greatly influence the rennet-induced coagulation of milk including the type of milk. The use of homogenised milk for the manufacture of Cheddar cheese is known to produce curds that tend to retain excess moisture and that have an increased propensity to develop rancid flavours due to lipolysis (Zamora, Ferragut, Jaramillo, Guamis, & Trujillo, 2007). However, the use of homogenised milk can provide valuable insight into the impact of cheese processing conditions. Raw milk can be partially homogenised by unit operations such as pumping and separation prior to cheese making. The microstructure of the gel formed from homogenised milk therefore provides a useful comparison to the microstructure formed by unhomogenised milk during Cheddar manufacture.

The microstructure of the curd collected just prior to draining is important as it may affect the amount of fat lost in the whey. The microstructure of the final cheese is also important and is known to affect the texture and flavour of cheese (Everett & Auty, 2008). The cryo SEM and CLSM were therefore used to track the evolution of product microstructure using samples from key points during Cheddar manufacture.

Image analysis was used to quantify the porosity from cryo SEM and CLSM images and these data are presented in Table 1. The grey-scale nature of cryo SEM images makes image analysis of the fat globules difficult. Fat globules can be readily identified in CLSM images due to the use of protein and lipid specific stains, so fat globule data are reported for CLSM images only. Previously, the fat globule size distribution obtained using CLSM by this method was found to produce a fat globule distribution similar to that obtained using light scattering (Ong et al., 2010), illustrating the usefulness of this technique.

The microstructure of the gel, cooked curd and cheese observed using cryo SEM (Figs. 4 and 5) largely resembles the structure observed for stained samples by CLSM (Figs. 6 and 7). The porosity data measured for the gel and cooked curd by cryo SEM were also comparable to those obtained by CLSM (Table 1). One advantage of Cryo SEM as a technique to assess microstructure is that cryo SEM images have higher resolution without the need for artificial staining. This may be essential for samples where differential staining between the whey and casein matrix is not possible, due to

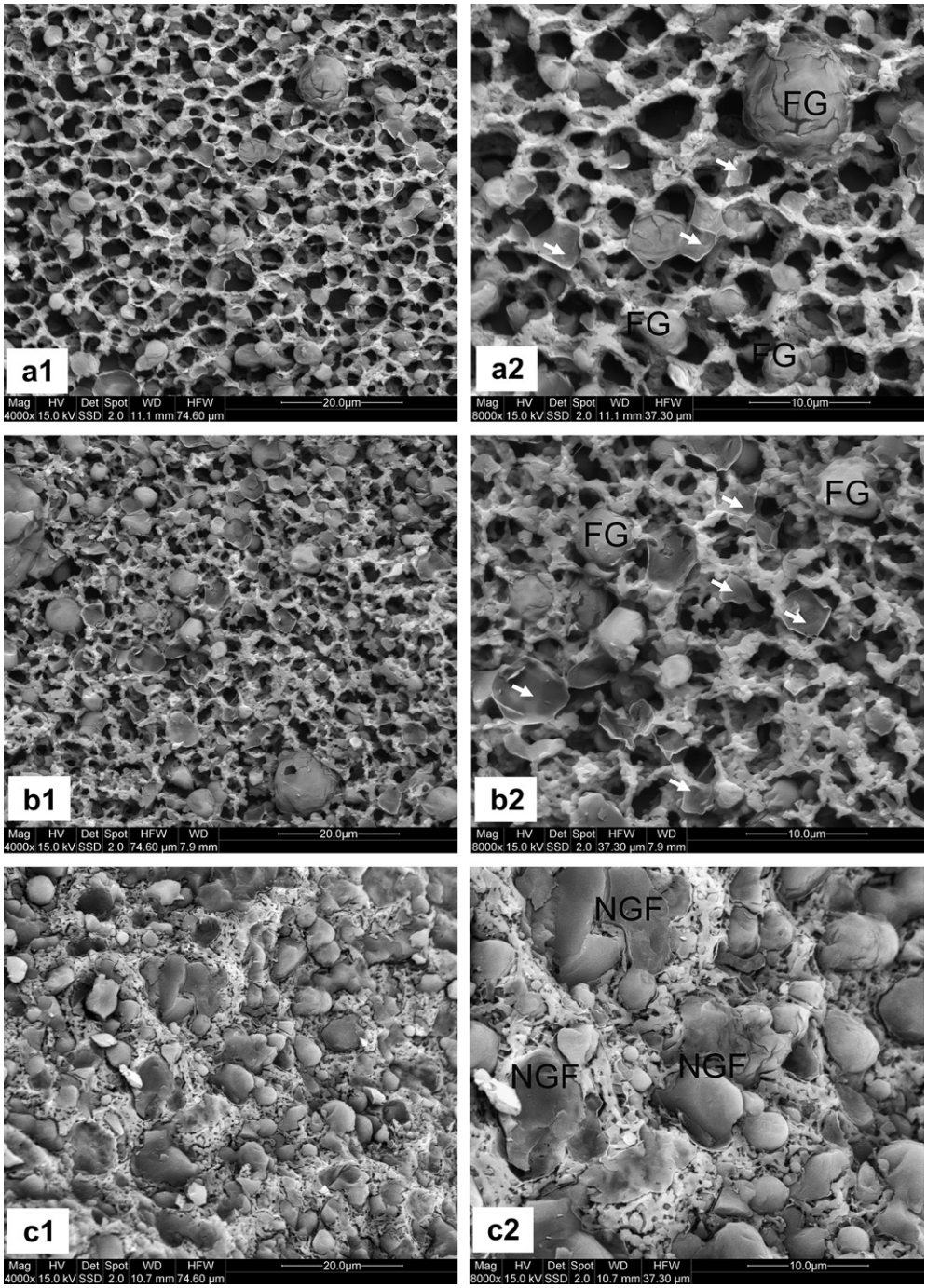


Fig. 4. Cryo scanning electron microscopy images of (a) the gel, (b) the cooked curd and (c) cheese prepared from unhomogenised milk. The scale bars are 20 μm (a1, b1, c1) and 10 μm (a2, b2, c2) in length. Images were captured using a solid state backscatter electron detector. Arrows indicate remnant fat from globules partially removed during sample preparation. This remnant fat possibly contains the milk fat globule membrane. FG = fat globule and NGF = non globular fat.

similar protein concentrations. In addition, the aqueous serum that covers the pores in samples prepared for cryo SEM is sublimed enhancing image clarity. This serum remains in CLSM images and contributes fluorescence to these images (Figs. 6 and 7). However, the observation of samples using cryo SEM does not allow microstructure differentiation based on chemical composition, leading to the difficulty observing and quantifying fat globules discussed above. It is notable that the cryo SEM images of cheese (Figs. 4 and 5) resemble cryo SEM images reported previously for full fat Cheddar cheese (Hassan & Awad, 2005). Sample preparation was largely similar but greater structural detail was visible in Figs. 4 and 5, perhaps due to the thinner coating of Au/Pd alloy used in this study. Details of the microstructure of the gel, curd and cheese made using homogenised or unhomogenised milk are discussed in the following section. A comparison of the images for samples made from unhomogenised or homogenised milk also allows the effect of homogenisation to be observed and quantified.

3.2.1. *Microstructure of rennet-induced gel*

The microstructure of gels formed from unhomogenised (Figs. 4 and 6) and homogenised milk (Figs. 5 and 7) were different. Fat globules within the gel prepared from unhomogenised milk were

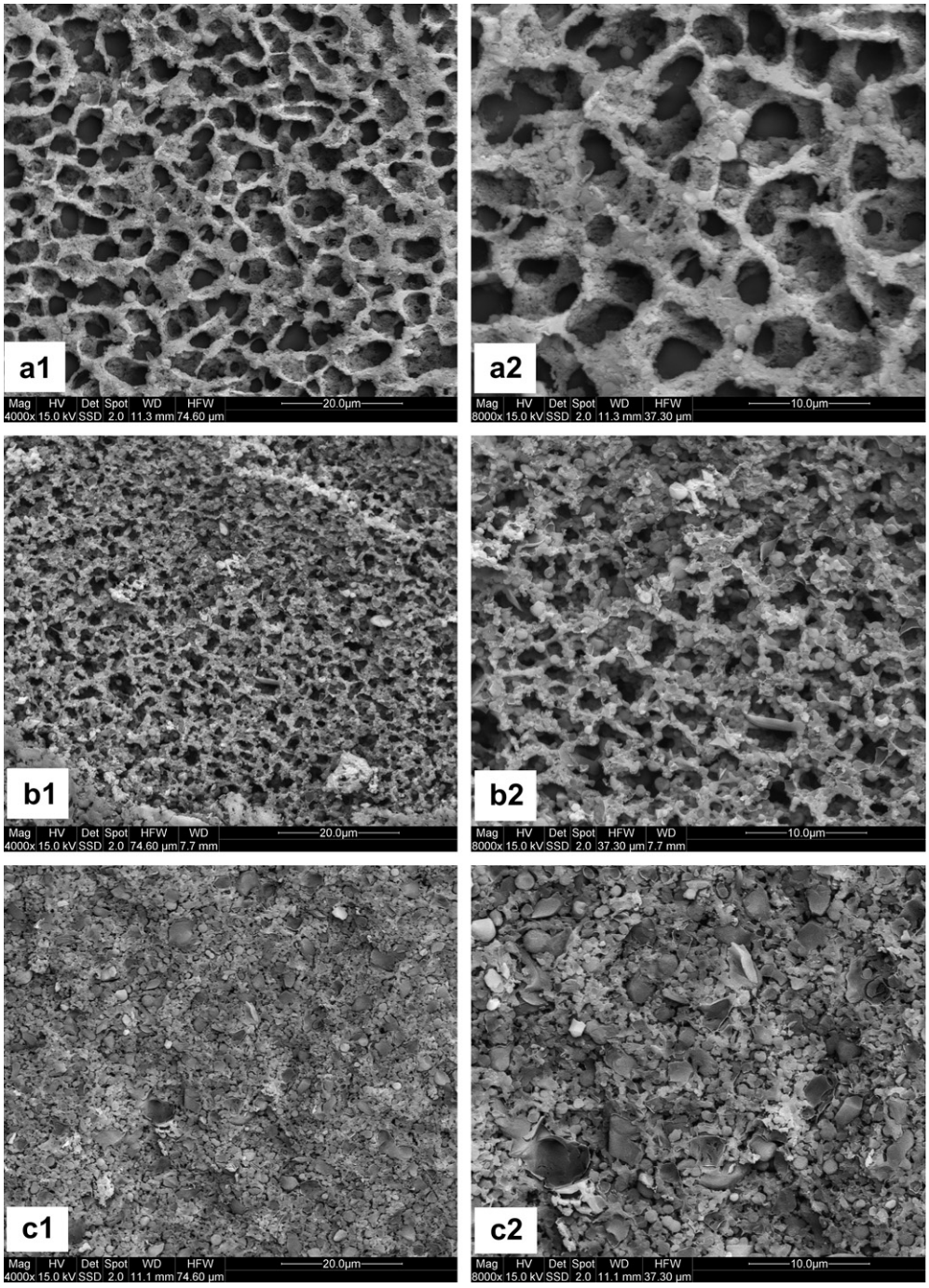


Fig. 5. Cryo scanning electron microscopy images of (a) the gel, (b) the cooked curd and (c) cheese prepared from homogenised milk. Images were captured using a solid state backscatter electron detector. The scale bars are 20 μm (a1, b1, c1), and 10 μm (a2, b2, c2) in length.

bigger and more readily observed (Figs. 4a and 6a) as compared to fat globules within homogenised milk samples (Figs. 5a and 7a). Image analysis indicated that the spherical fat globules in the CLSM images have a number-area mean diameter $D_{FG}[2,0]$ of 2.82 ± 0.16 μm and 1.28 ± 0.48 μm in the gels prepared from unhomogenised and homogenised milk respectively.

The CLSM images show that the majority of fat globules in the gel prepared from unhomogenised milk are located in the serum pores of the protein network (Fig. 6a). Some of these fat globules appear to contact the protein network in both CLSM (Fig. 6a) and cryo SEM images (Fig. 4a) but also protrude into the serum pores (Figs. 4a and 6a). Fewer fat globules were observed in the cryo SEM images compared to in CLSM images and some fat globules may have detached during freeze fracture. Interestingly, some of the fat globules lost during this process left behind what was possibly the milk fat globule membrane (Fig. 4a, indicated by the arrow), suggesting that chemical bonds may exist between the native fat globule membrane components and the protein matrix, although further investigation is required to confirm these potential interactions.

The position of fat globules in the gel prepared from homogenised milk is in striking contrast to that from unhomogenised milk where the fat globules appear well embedded within the protein network in both CLSM and cryo SEM images (Figs. 7a and 5a). The

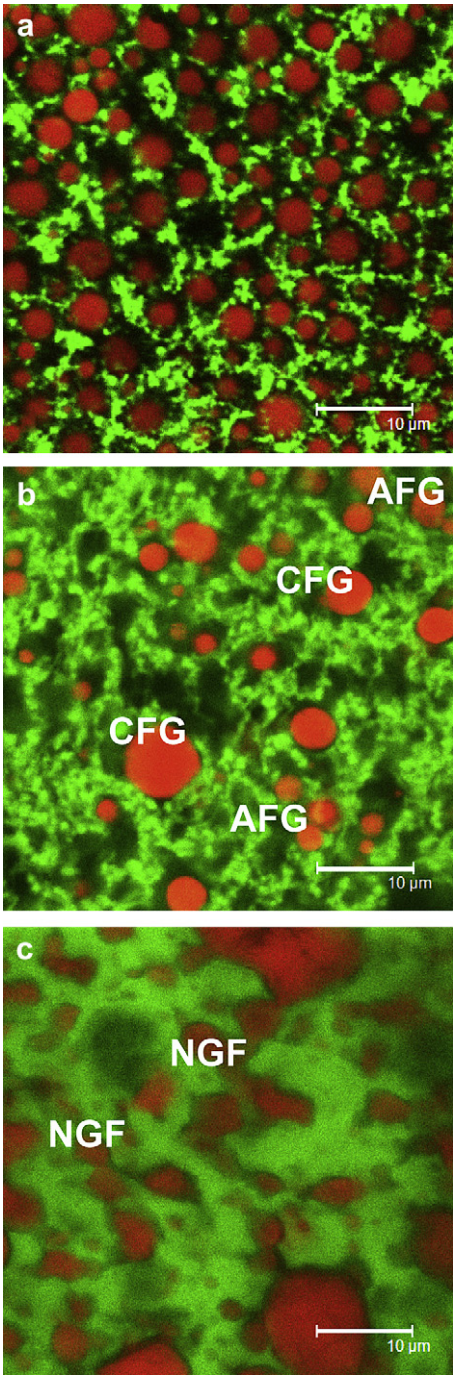


Fig. 6. Confocal micrographs showing the microstructure of (a) the gel, (b) the cooked curd and (c) cheese prepared from unhomogenised milk. The Nile red stained fat appears red and the fast green FCF stained protein appears green in these images. AFG = aggregates of fat globules, CFG = coalesced fat globules, NGF = non globular fat. The scale bars are 10 μm in length (For interpretation of the references to colour in this figure legend, the reader is referred to the web version of this article).

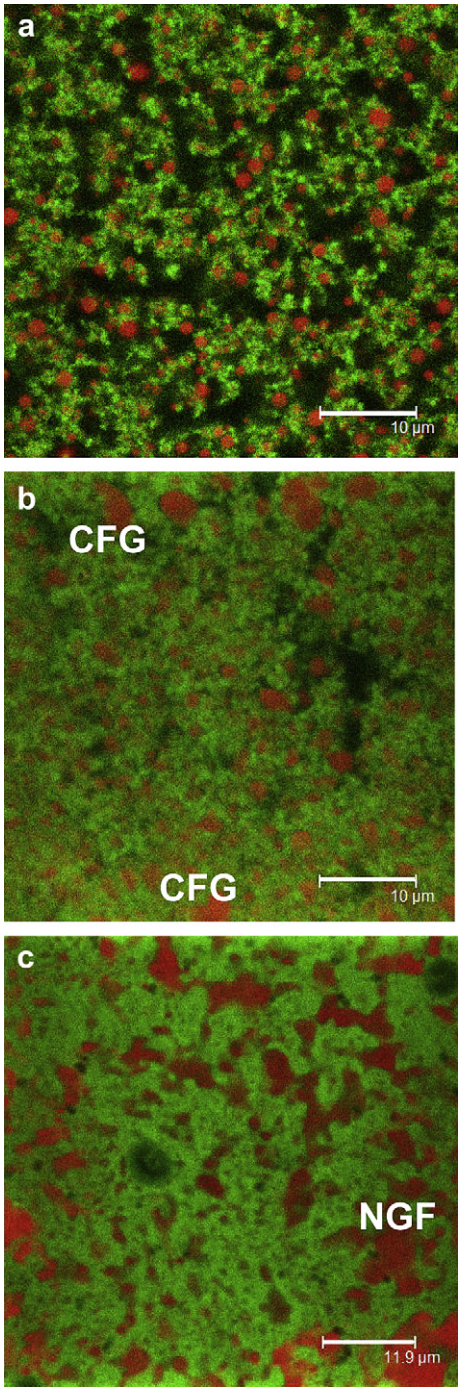


Fig. 7. Confocal micrographs showing the microstructure of (a) the gel, (b) the cooked curd and (c) cheese prepared from homogenised milk. The Nile red stained fat appears red and the fast green FCF stained protein appears green in these images. CFG = coalesced fat globules, NGF = non globular fat. The scale bars are 10 μm (a–b) or 11.9 μm (c) in length (For interpretation of the references to colour in this figure legend, the reader is referred to the web version of this article).

presence of the recombined fat globule membrane (RFGM) in the homogenised milk may be responsible for the inclusion of these fat globules within the protein matrix. Previous studies reported that homogenisation can cause major physical changes in the size of the fat globule and the native milk fat globule membrane (Cho, Lucey, & Singh, 1999; Ong et al., 2010). Milk caseins are able to absorb onto the fat globule surface (Ong et al., 2010; Sharma & Dalgleish, 1993) and this protein layer, frequently denoted the RFGM, enables the newly formed fat globules to behave as pseudo-protein particles that can interact with the casein micelles becoming an integral part of the casein matrix during coagulation (Lopez, 2005). The smaller size of homogenised globules may also aid their inclusion within the matrix. The fat globules in the homogenised milk thus become an important structural constituent.

The difference in gel microstructure for samples made from unhomogenised and homogenised milk is obvious, as the inclusion of fat globules in the casein matrix formed from homogenised milk

Table 1
Porosity of the gel, cooked curd and cheese samples obtained using cryo SEM and CLSM.[c]

Sample	Cryo SEM		CLSM	
	Unhomogenised milk	Homogenised milk	Unhomogenised milk	Homogenised milk
Gel	0.55 ± 0.06^{aA}	0.51 ± 0.02^{aA}	0.50 ± 0.01^{aA}	0.55 ± 0.09^{aA}
Cooked curd	0.34 ± 0.03^{aB}	0.42 ± 0.06^{aB}	0.40 ± 0.03^{aB}	0.37 ± 0.05^{aB}
Cheese	0.13 ± 0.01^{aC}	0.06 ± 0.03^{bC}	0.14 ± 0.01^{aC}	0.04 ± 0.04^{bC}

[ab]The means within a single row with different superscripts are significantly different ($P < 0.05$).
[AB]The means within a single column with different superscripts are significantly different ($P < 0.05$).
[C] Micrographs were analysed using ImageJ. Porosity was calculated as the fraction of pore area with respect to the total sample area. Results are expressed as the mean ± the standard deviation ($n = 3$).

is known to soften the casein network (Cano-Ruiz & Richter, 1997). This reduced gel strength may also affect the ability of the curd particles to knit together during cheese manufacture and thereby increase the tendency of moulded curds to break easily or shatter during milling. This in turn may alter the functionality of the final cheese, with the cheese being more easily fractured, less elastic and more crumbly (Jana & Upadhyay, 1992). A further consequence may be the reduced ability of the protein network to contract and expel moisture during cooking, which is likely to affect the moisture content of the cheese. The moisture content of the cheeses made in this study were not analysed but in another study it was found that Mozzarella cheese made from homogenised milk had a higher moisture content than cheese made from unhomogenised milk (Rowney, Hickey, Roupas, & Everett, 2003).

Notably, the fat globules in the gel formed from both unhomogenised and homogenised milk are qualitatively smaller than the pores of the casein network. The size and the placement of fat globules within the casein network are critical to both gel properties and fat retention. Large native unprocessed milk fat globules have been observed to act as structure breakers leading to local disruption of the casein network in both rennet and acid induced gels (Michalski, Cariou, Michel, & Garnier, 2002). Large fat globules are also excluded from the small pores of the casein matrix and may be lost from the curd structure after cutting of gel (Everett & Auty, 2008). It is therefore important to understand the size and placement of fat globules to control fat loss into the whey stream during manufacturing.

3.2.2. *Microstructure of curd after cooking*

The para-casein micelles aggregated in samples from both unhomogenised and homogenised milk, following the cutting and cooking of curd at 38 °C. The cryo SEM images indicate that the protein matrix becomes more compact (Figs. 4b and 5b), consistent with the images obtained by CLSM (Figs. 6b and 7b). The aggregation of the para-casein micelles results in an overall contraction of the curd network and expulsion of whey. This contraction can be seen quantitatively by the significant decrease in porosity for cooked samples made from unhomogenised and homogenised milk compared to those in gel samples (Table 1). Image analysis of CLSM

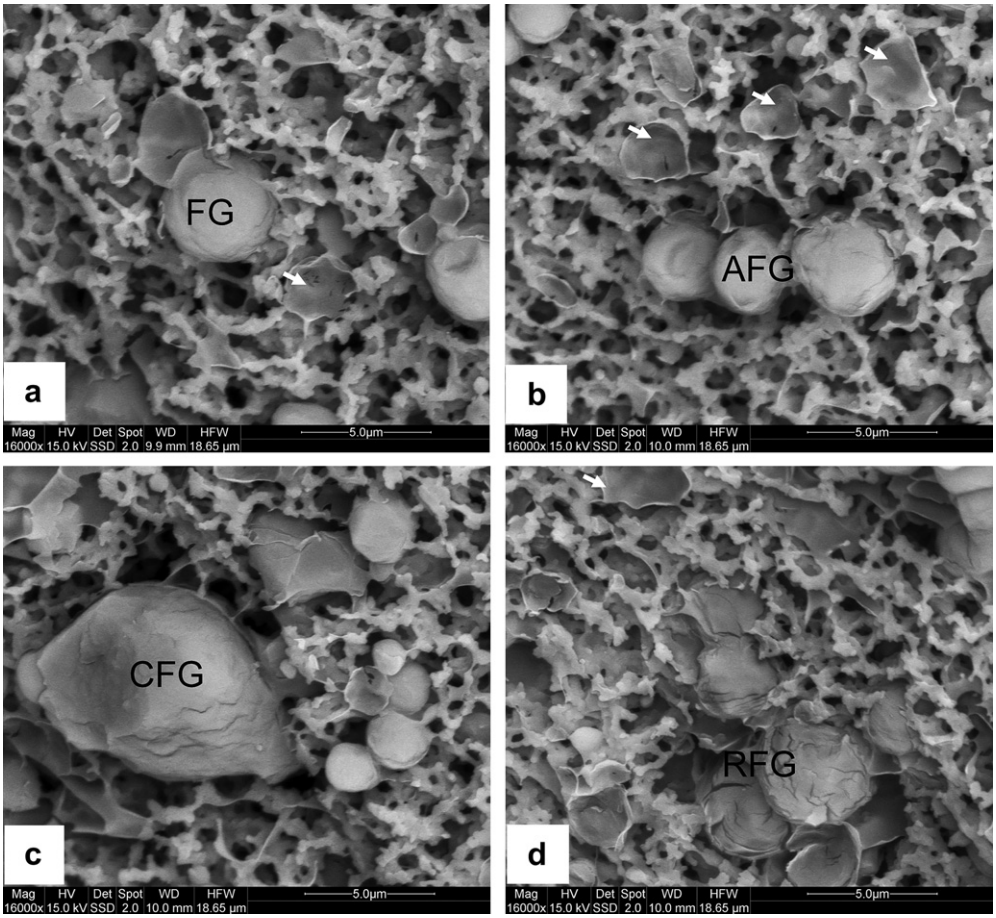


Fig. 8. Different fat globule structures within the cooked curd prepared from unhomogenised milk: (a) fat globule, FG; (b) aggregated fat globule, AFG; (c) coalesced fat globule, CFG; (d) fat globule artefact showing the rupture of fat globule (RFG) due to the high energy electron beam. Arrows indicate remnant fat from globules partially removed during sample preparation. Images were captured using a solid state backscatter electron detector. The scale bars are 5 µm in length.

images show that the heat during cooking also results in a significant increase in the size of the fat globules in cooked curd prepared from unhomogenised milk ($P < 0.05$, $D_{FG}[2,0] = 3.46 \pm 0.15$ μm following cooking) but not in cooked curd from homogenised milk ($D_{FG}[2,0] = 1.51 \pm 0.6$ μm). Interestingly, individual fat globules can still be observed within the curds prepared from both milk types after cooking.

Different possible structures for fat such as aggregated fat globules (AFG) and coalesced fat globules (CFG) could be observed after cooking. Fig. 8 indicates the different structure of fat globules observed within the cooked curd sample prepared from unhomogenised milk. A few fat globules were also observed to have ruptured (RFG, Fig. 8d) during the cryo SEM observation, possibly due to the high-energy electron beam. Changes in the structure of the fat globules after cooking were less obvious in the homogenised milk sample.

3.2.3. Microstructure of cheese

The density of the protein matrix continued to increase after cheddaring and pressing. The porosity of the curd produced from unhomogenised and homogenised milk was further reduced after this step (Table 1). Thicker protein fibres were clearly visible on the cryo SEM and CLSM micrographs of the cheese (Figs. 4c, 5c, 6c and 7c). These are likely to result from the slow flow of curd induced during the cheddaring process, where slabs of the warm curd are piled in the cheese vat at 38 °C. This curd flow increases as the pH decreases towards the end of the cheddaring process (Lucey & Fox, 1993), forcing the casein to fuse into thicker fibres that result in a loss of micelle identity. During pressing, the casein fibres further fuse together, closing most of the gaps in the curd microstructure.

The heat treatment applied during cheddaring also causes further aggregation and the coalescence of further fat globules. Finally, pressing results in the disruption of fat globules. The majority of fat globules in Figs. 4c, 5c, 6c and 7c no longer resemble spherical globules. Image analysis of the CLSM images indicates that the fat globules have a number-area mean diameter $D_{FG}[2,0]$ of 3.61 ± 0.35 μm and 3.48 ± 0.32 μm in the cheese prepared from unhomogenised and homogenised milk respectively. The cheese made from unhomogenised milk appears to have a greater quantity of free fat or non globular fat (NGF, Figs. 4c and 6c) compared to cheese made from homogenised milk (Figs. 5c and 7c). Such NGF is typically fat dispersed in the casein matrix and is not protected by the milk fat globule membrane (Lopez et al., 2007).

The microstructure of the cheese made from unhomogenised and homogenised milk is clearly different. This difference will potentially affect the functional properties of the cheese such as meltability. Cheese melting involves a series of steps; the fat melts, followed by the collapse of the cheese matrix due to reduced support from the fat globules (Lefevere, Dewettinck, & Huyghebaert, 2000). The size of the fat globules and interactions between these globules and/or free fat within the casein matrix may play a dominant role in determining meltability (Rowney, Roupas, Hickey & Everett, 2003). The collapse of the casein matrix during melting may occur faster in cheese from homogenised milk compared to in cheese from unhomogenised milk, as a result of the smaller distances between the fat globules and thinner casein strands (Michalski et al., 2003).

4. Conclusion

The visualisation of product microstructure during cheese making is complex due to the wide range of structural and chemical changes that occur during manufacture and the wide range of parameters that can be used during imaging. Our results show that sample preparation for observation by cryo SEM requires optimisation to minimise the formation of artefacts such as the growth of large ice crystals and ice recrystallisation or secondary nucleation during specimen transfer, freeze etching, coating and sample observation.

Qualitatively, the microstructure of samples observed by cryo SEM using optimised conditions was similar to the structure observed using CLSM, indicating the absence of damaging ice crystals. Despite the risk of possible artefacts, cryo-fixation is preferable to chemical fixation in that the artefacts are fewer and easier to interpret, although image analysis of fat globules is not possible with this method. CLSM provides similar structural information to Cryo SEM but allows the chemical composition to be visualised through staining techniques. It is possible to assess aspects of product microstructure using either Cryo SEM or CLSM alone, depending on the structural information required. Together these techniques provide a complementary and more thorough assessment of product microstructure that can be applied to a wide range of cheeses and other hydrated food products.

Our results show that cryo SEM can be used to image structural changes that occur in the gel, curd and cheese during the manufacture of Cheddar cheese. CLSM provided complementary insights into the evolution of cheese microstructure. Differences in the microstructure of the samples prepared from unhomogenised and homogenised milk also provide insight into the effect of milk processing on product microstructure and the possible changes in downstream properties and functionality of the cheese product.

Acknowledgements

This work was funded by Dairy Innovation Australia Limited. The authors would like to thank the Bio21 Molecular Science & Biotechnology Institute and the Particulate Fluids Processing Centre, a Special Research Centre of the Australian Research Council at The University of Melbourne, for access to equipment. We would also like to thank Murray Goulburn, Warrnambool Cheese and Butter Factory, National Foods and Burra Foods for their involvement. We appreciate the technical input from Mr Roger Curtain (Bio21 Molecular Science and Biotechnology Institute, The University of Melbourne) and his help operating the scanning electron microscope in cryo mode.

Appendix. Supplementary material

Supplementary data related to this article can be found online at doi:10.1016/j.lwt.2010.12.026.

References

Abeysekera, R. M., & Robards, A. W. (1995). Freeze fracture artifacts: how to recognize and avoid them. In N. J. Severs, & D. M. Shotton (Eds.), *Rapid freezing, freeze fracture and deep etching* (pp. 70–87). New York: Willey-Liss Inc.

Amatayakul, T., Sherkat, F., & Shah, N. P. (2006). Physical characteristics of set yoghurt made with altered casein to whey protein ratios and EPS-producing starter cultures at 9 and 14% total solids. *Food Hydrocolloids, 20*, 314–324.

Auty, M. A. E., Twomey, M., Guinee, T. P., & Mulvihill, D. M. (2001). Development and application of confocal scanning laser microscopy methods for studying the distribution of fat and protein in selected dairy products. *Journal of Dairy Research, 68*, 417–427.

Bowland, E. L., & Foegeding, E. A. (2001). Small strain oscillatory shear and microstructural analyses of a model processed cheese. *Journal of Dairy Science, 84*, 2372–2380.

Cano-Ruiz, M. E., & Richter, R. L. (1997). Effect of homogenization pressure on the milk fat globule membrane proteins. *Journal of Dairy Science, 80*, 2732–2739.

Cho, Y. H., Lucey, J. A., & Singh, H. (1999). Rheological properties of acid milk gels as affected by the nature of the fat globule surface material and heat treatment of milk. *International Dairy Journal, 9*, 537–545.

Davy, J. G., & Branton, D. (1970). Subliming ice surfaces: freeze-etch electron microscopy. *Science, 168*, 1216–1218.

Donald, A. M. (2003). The use of environmental scanning electron microscopy for imaging wet and insulating materials. *Nature Materials, 2*, 511–516.

Everett, D. W. (2007). Microstructure of natural cheese. In A. Y. Tamime (Ed.), *Structure of dairy products* (pp. 170–201). London, UK: Blackwell Publishing.
Everett, D. W., & Auty, M. A. E. (2008). Cheese structure and current methods of analysis. *International Dairy Journal, 18*, 759–773.
Fallico, V., Tuminello, L., Pediliggieri, C., Horne, J., Carpino, S., & Licitra, G. (2006). Proteolysis and microstructure of Piacentinu Ennese cheese made using different farm technologies. *Journal of Dairy Science, 89*, 37–48.
Gilkey, J., & Staehelin, L. (1986). Advances in ultrarapid freezing for the preservation of cellular ultrastructure. *Journal of Electron Microscopy, 166*, 207–218.
Hassan, A. N., & Awad, S. (2005). Application of exopolysaccharide-producing cultures in reduced-fat cheddar cheese: cryo-scanning electron microscopy observations. *Journal of Dairy Science, 88*, 4214–4220.
Hassan, A. N., Frank, J. F., & Elsoda, M. (2003). Observation of bacterial exopolysaccharide in dairy products using cryo-scanning electron microscopy. *International Dairy Journal, 13*, 755–762.
Heilig, A., Göggerle, A., & Hinrichs, J. (2009). Multiphase visualisation of fat containing [beta]-lactoglobulin-[kappa]-carrageenan gels by confocal scanning laser microscopy, using a novel dye, V03-01136, for fat staining. *LWT - Food Science and Technology, 42*, 646–653.
Herbert, S., Bouchet, B., Riaublanc, A., Dufour, E., & Gallant, D. J. (1999). Multiple fluorescence labelling of proteins, lipids and whey in dairy products using confocal microscopy. *Le Lait, 79*, 567–575.
Impoco, G., Carrato, S., Caccamo, M., Tuminello, L. & Licitra, G. (2006). Image analysis methods for industrial application: quantitative analysis of cheese microstructure using SEM imagery. In *ADSA - ASAS Joint Annual Meeting*: Minneapolis, USA.
James, B. (2009). Advances in "we" electron microscopy techniques and their application to the study of food structure. *Trends in Food Science & Technology, 20*, 114–124.
Jana, A. H., & Upadhyay, K. G. (1992). Homogenization of milk for cheesemaking - a review. *Australian Journal of Dairy Technology, 47*, 72–79.
Kalab, M., Allan-Wojtas, P., & Miller, S. S. (1995). Microscopy and other imaging techniques in food structure analysis. *Trends in Food Science & Technology, 6*, 177–186.
Kalab, M., & Harwalkar, V. R. (1973). Milk gel structure. I. Application of scanning electron microscopy to milk and other food gels. *Journal of Dairy Science, 56*, 835–842.
Kasas, S., Dumas, G., Dietler, G., Catsicas, S., & Adrian, M. (2003). Vitrification of cryoelectron microscopy specimens revealed by high-speed photographic imaging. *Journal of Microscopy, 211*, 48–53.
Kheadr, E. E., Vachon, J. F., Paquin, P., & Fliss, I. (2002). Effect of dynamic high pressure on microbiological, rheological and microstructural quality of cheddar cheese. *International Dairy Journal, 12*, 435–446.
Kimber, A. M., Brooker, B. E., Hobbs, D. C., & Prentice, J. M. (1974). Electron microscope studies of the development of structure in cheddar cheese. *Journal of Dairy Research, 41*, 389–396.
Kuoa, M., & Gunasekaran, S. (2009). Effect of freezing and frozen storage on microstructure of mozzarella and pizza cheeses. *LWT - Food Science and Technology, 42*, 9–16.
Lagaude, A., Fernandez, L., Cuq, J. L., & Marchesseau, S. (2004). Characterization of curd formation during the rennet coagulation of milk by an optical microscopic method. *International Dairy Journal, 14*, 1033–1039.
Lefevere, I., Dewettinck, K., & Huyghebaert, A. (2000). Cheese fat as a driving force in cheese flow upon melting. *Milchwissenschaft, 55*, 563–566.
Lopez, C. (2005). Focus on the supramolecular structure of milk fat in dairy products. *Reproduction Nutrition Development, 45*, 497–511.
Lopez, C., Camier, B., & Gassi, J. (2007). Development of the milk fat microstructure during the manufacture and ripening of emmental cheese observed by confocal laser scanning microscopy. *International Dairy Journal, 17*, 235–247.
Lorén, N., Langton, M., & Hermansson, A. M. (2007). Confocal fluorescence microscopy (CLSM) for food structure characterisation. In D. J. McClements (Ed.), *Understanding and controlling the microstructure of complex foods* (pp. 232–260). Cambridge, England: Woodhead Publishing Limited.
Lucey, J. A., & Fox, P. F. (1993). Importance of calcium and phosphate in cheese manufacture: a review. *Journal of Dairy Science, 76*, 1714–1724.
McMahon, D. J., Fife, R. L., & Oberg, C. J. (1999). Water partitioning in mozzarella cheese and its relationship to cheese meltability. *Journal of Dairy Science, 82*, 1361–1369.
Mellema, M., Walstra, P., can Opheusden, J. H. J., & van Vliet, T. (2002). Effects of structural rearrangements on the rheology of rennet-induced casein particle gels. *Advances in Colloid and Interface Science, 98*, 25–50.
Merrill, R. K., Oberg, C. J., McManus, W. R., Kalab, M., & McMahon, D. J. (1996). Microstructure and physical properties of a reduced fat mozarella cheese made using Lactobacillus casei ssp. casei adjunct culture. *LWT - Food Science and Technology, 29*, 721–728.
Michalski, M. C., Cariou, R., Michel, F., & Garnier, C. (2002). Native vs. damaged milk fat globules: membrane properties affect the viscoelasticity of milk gels. *Journal of Dairy Science, 85*, 2451–2461.
Michalski, M. C., Gassi, J. Y., Famelart, M. H., Leconte, N., Camier, B., & Michel, F. (2003). The size of native milk fat globules affects physico-chemical and sensory properties of Camembert cheese. *Le Lait, 83*, 131–143.
Mistry, V. V., Hassan, A. N., & Acharya, M. R. (2006). Microstructure of pasteurized process cheese manufactured from vacuum condensed and ultrafiltered milk. *Le Lait, 86*, 453–459.
Mounsey, J. S., & O'Riordan, E. D. (2008). Influence of pre-gelatinised maize starch on the rheology, microstructure and processing of imitation cheese. *Journal of Food Engineering, 84*, 57–64.
Noronha, N., Duggan, E., Ziegler, G. R., Stapleton, J. J., O'Riordan, E. D., & O'Sullivan, M. (2008). Comparison of microscopy techniques for the examination of the microstructure of starch-containing imitation cheeses. *Food Research International, 41*, 472–479.
Oiseth, S. K., & McKinnon, I. R. (2006). Confocal laser scanning microscopy studies of the molecular structure of cheese curd. *Australian Journal of Dairy Technology, 61*, 167–169.
Ong, L., Dagastine, R. R., Kentish, S. E., & Gras, S. L. (2010). The effect of milk processing on the microstructure of the milk fat globule and rennet induced gel observed using confocal laser scanning microscopy. *Journal of Food Science, 75*, E135–E145.
Rawle, A. (2002). The importance of particle sizing to the coatings industry Part 1: particle size measurement. *Advances in Colour Science and Technology, 5*, 1–12.
Riberoa, G. G., Rubioloa, A. C., & Zorrilla, S. E. (2009). Microstructure of mozzarella cheese as affected by the immersion freezing in NaCl solutions and by the frozen storage. *Journal of Food Engineering, 91*, 516–520.
Rowney, M. K., Hickey, M. W., Roupas, P., & Everett, D. W. (2003). The effect of homogenization and milk fat fractions on the functionality of mozzarella cheese. *Journal of Dairy Science, 86*, 712–718.
Rowney, M., Roupas, P., Hickey, M. W., & Everett, D. W. (2003). The effect of compression, stretching, and cooking temperature on free oil formation in mozzarella curd. *Journal of Dairy Science, 86*, 449–456.
Sartori, N., Richter, K., & Dubochet, J. (1993). Vitrification depth can be increased more than 10-fold by high pressure freezing. *Journal of Microscopy, 172*, 55–61.
Severs, N. J., Terence, M. N., & Shotton, D. M. (1995). A practical introduction to rapid freezing techniques. In N. J. Severs, & D. M. Shotton (Eds.), *Rapid freezing, freeze fracture and deep etching* (pp. 31–49). New York: Willey-Liss Inc.
Sharma, S. K., & Dalgleish, D. G. (1993). Interactions between milk serum proteins and synthetic fat globule membrane during heating of homogenised whole milk. *Journal of Agricultural and Food Chemistry, 41*, 1407–1412.
Yamada, N., Nagano, M., Murakami, S., Ikeuchi, M., Oho, E., Baba, N., et al. (1983). Preparation for observation of fine structure of biological specimen by high resolution SEM. *Journal of Electron Microscopy, 32*, 321–330.
Yiu, S. H. (1985). A fluorescence microscopic study of cheese. *Food Microstructure, 4*, 99–106.
Zamora, A., Ferragut, V., Jaramillo, P. D., Guamis, B., & Trujillo, A. J. (2007). Effects of ultra-high pressure homogenization on the cheese-making properties of milk. *Journal of Dairy Science, 90*, 13–23.
Zisu, B., & Shah, N. P. (2005). Textural and functional changes in low-fat mozzarella cheeses in relation to proteolysis and microstructure as influenced by the use of fat replacers, pre-acidification and EPS starter. *International Dairy Journal, 15*, 957–972.